PFG−NMR Techniques Provide a New Tool for Continuous Investigation of the Evolution of the Casein Gel Microstructure after Renneting

Steven Le Feunteun and François Mariette*

Cemagref, Food Process Engineering Research Unit, CS 64426, 17 avenue de Cucillé, 35044 Rennes, Cedex, France

Received October 8, 2007; Revised Manuscript Received December 13, 2007

ABSTRACT: The self-diffusion of water and a small and a large poly(ethylene glycol) (PEG) were monitored during the sol−gel transition of a casein system induced by chymosin action using pulsed field gradient (PFG) NMR techniques throughout the coagulation process. Rheological measurements revealed that the diffusion rate of the molecules studied was unaffected by the establishment of a network. However, different evolutions occurred during the gel aging phase, depending on the size of the diffusing molecule. The diffusion coefficient of water remained constant whereas the diffusivity of the small PEG decreased and that of the large PEG increased. Scanning electron microscopy images showed that all these findings could be explained by the progressive compaction of the casein network caused by the occurrence of structural rearrangements. This study demonstrates the sensitivity of probe diffusion to structural changes in casein gels and also the potential of PFG−NMR techniques to reveal dynamic information on evolving systems at different length scales.

Introduction

Casein is the main milk protein component. It exists in milk as a suspension of large spherical particles called casein micelles. These colloidal particles can be destabilized in different ways, but in the manufacture of most cheese varieties, the critical first step is the gelation of milk by addition of rennet. The main active component in rennet, chymosin, causes the casein particles to aggregate and form a gel by an enzymatic reaction. Once a three-dimensional casein network is formed, it progressively undergoes structural modifications such as fusion and compaction of the casein particles, which can lead to micro- and macrosyneresis, i.e., whey separation.[1]

Various parameters such as chymosin and casein concentrations, pH and temperature directly influenced the dynamics of the coagulation process.[2−10] Depending on these conditions, the gel microstructure and its rheological properties, which are very important attributes of the product, can therefore be very different. The extent of the structural rearrangements that occur during the aging of the fresh gel seems to be of primary importance,[1,6] but although it is possible to highlight their effects, no ideal technique exists to investigate their dynamics.

Probe diffusion studies have proved to be very sensitive not only to changes in the microstructure of a great number of synthetic polymer matrices[11−22] but also to the coagulation of alginate solutions,[23,24] of sugar-based samples,[11,25,26] and of milk protein systems such as β-lactoglobulin,[27] whey protein,[28,29] and casein micelle[30] solutions. In casein matrices, the diffusion rates of large poly(ethylene glycol) (PEG) probes are enhanced after coagulation,[30] and we demonstrated in a recent study that the size of these increases depends on the final gel microstructure.[31] This could be explained by considering that the diffusion of large probes is very sensitive to the extent of the casein aggregate compaction and thus to the extent of certain rearrangement processes. However, as in all the studies quoted above, the diffusion of a molecule was measured at equilibrium, before and after the perturbation of the system. This method cannot provide any dynamic information on the evolution of the sample microstructure although the modifications of the matrix in reaction to the perturbation can be very progressive. This is precisely the case when casein suspensions are coagulated by addition of chymosin and/or acidifying agent.

In the present study, we designed an original method to investigate how and when probe diffusion rates vary during the coagulation induced by chymosin action. Self-diffusion measurements were repeated throughout the coagulation process by means of pulsed field gradient (PFG) NMR techniques. This was possible because NMR techniques are noninvasive (i.e., a sample can be analyzed an unlimited number of times) and because a diffusion coefficient can be obtained in a few minutes. This method enabled us to reveal dynamic information on the sample microstructure modifications during the sol−gel transition. This study therefore constitutes a new illustration of the potential of probe diffusion measurements to reveal structural changes in complex and evolving matrices. In addition, a WATERGATE scheme was used to suppress the water signal when studying the diffusion of probes. All casein samples were therefore prepared without resorting to the use of heavy water, thus permitting work on realistic products.

The diffusion coefficients of water and a small and a large PEG were followed during the course of the coagulation according to this procedure. The evolution of probe diffusion rates was related to dynamic rheological data and stiffness measurements to characterize the key steps of gel formation. In addition, scanning electron microscopy (SEM) images taken at different times after addition of the enzyme illustrated the changes in gel microstructure during aging. We showed that different evolutions in the diffusion rates of the molecules studied could be explained with a single interpretation based on compaction of the casein network. The results also demonstrate that probe diffusion measurements during coagulation of a casein sample can contribute to better rationalization of dairy processes.

* Corresponding author. Telephone: 33 (0)223482121. Fax: 33 (0)-223482115. E-mail: Francois.Mariette@cemagref.fr.

10.1021/ma702246m CCC: $40.75
Published on Web 01/26/2008

Table 1. Composition of Micellar Casein Powder

	micellar casein powder (%)
total solids (g/kg)	100
total nitrogen matter (g/kg)	90.7
non-casein nitrogen (g/kg)	5.7
non-protein nitrogen (g/kg)	0.6
calcium (g/kg)	2.9
ash (g/kg)	8.1
pure caseins (g/kg)	85.0

Materials and Methods

Materials. Native phosphocaseinate powder (INRA, Rennes, France) was used. The powder composition is summarized in Table 1. The PEG polymers were obtained from Polymer Laboratories (Marseille, France), with average molecular masses of 620 and 96750 g/mol. Both polymers had the same low polydispersity index of 1.06 as indicated by the suppliers. All polymers, sodium azide (NaN_3) (Merck, Darmstadt, Germany) and sodium chloride (NaCl) were used without further purification. The chymosin solution used was Chymax-Plus purchased from Chr-Hansen (Arpajon, France).

Preparation of Native Phosphocaseinate Suspension (NPCS). The aqueous phase used for the reconstitution consisted of H_2O, with 0.1 M NaCl and 0.2% (w/w) NaN_3 to prevent bacterial growth. Native phosphocaseinate powder (21.0% w/w) was added to the aqueous phase and the solution was vigorously stirred at room temperature for 36 h to ensure total rehydration of the powder. After this period, 0.1% (w/w) of PEG was added to casein suspensions for the NMR experiments, regardless of molecular weights. The dry matter of all casein suspensions was controlled by measuring variations in weight after drying in an oven for 24 h at 100 °C. Casein concentrations were calculated from values of dry matter in each casein suspension and the pure casein percentage of the dry matter (85.0%, see Table 1). The casein suspension concentrations in all samples were 16.75 ± 0.35 g of casein for 100 g of H_2O, and the pH was 6.80 (Schott, pH combination electrode type No N6280, Germany).

Enzymatic Coagulation. A chymosin dilution (1 mL in 99.0 g of distilled water) was always prepared and stored at 4 °C approximately 20 min before each inoculation to allow more accurate dosage. To start the coagulation process, the chymosin dilution was added to the casein suspension at the proportion of 700 μL for 100 g of NPCS. A chronometer was started at the same time ($t = 0$ s) and the solution was vigorously stirred for 3 min. Samples were then rapidly prepared for NMR and dynamic rheological measurements, whereas for SEM and puncture experiments, samples were stored at 20 °C before analysis. No shrinkage of the gel was observed during the time scale of the experiments.

Dynamic Rheological Measurements. The viscoelastic properties of the enzymatic gel were studied with a controlled stress rheometer (Rheostress RS150, Haake, Germany) using a double gap cylinder sensor (DG41). The temperature was maintained at 20 °C and the surface of the sample was covered with silicone oil to prevent evaporation. The storage modulus (G'), loss modulus (G'') and phase angle ($\delta = \text{tangent}^{-1}(G''/G')$) were recorded at a frequency of 1 Hz and the rheometer was programed to adjust the stress automatically to provide a strain of 0.5%, which was found to be within the linear viscoelastic region of the sample.

Puncture Tests. The penetration measurements were performed with an Instron Universal Testing Machine 5500 (Instron Ltd., France) monitored by the Merlin software. A flat end puncture probe with a diameter of 12.5 mm was pushed into the sample at a speed of 100 mm/min. The depth of penetration into the sample was 8 mm and the data sampling rate was 50 points per second. The stiffness (slope of the linear part of the curve, representing the elastic deformation, N/mm) and the hardness (strength at the ultimate depth, N), or the strength at fracture (N) when it occurred, were calculated.

Scanning Electron Microscopy (SEM). At different times after the addition of chymosin, small cubes (5 × 5 × 5 mm) were cut out from the gels and immersed for 48 h at 20 °C in a sodium cacodylate buffer, pH 7.2, with 2.5% (v/v) glutaraldehyde. Samples were rinsed several times with distilled water before being dehydrated in a graded ethanol series (10−30−50−70−80−90−95−100% (v/v)) in 20 min steps and finally conserved in acetone (purity above 99.9%). Samples were then critical-point dried through CO_2 in a critical-point drier (CPD 010, Balzers Union Ltd., Liechtenstein). Dried samples were fractured, mounted onto specimen stubs, gold coated and analyzed microscopically using a scanning electron microscope (Jeol JSM 6301F) operated at an acceleration voltage of 9 kV. The images were produced by CMEBA (France, Rennes).

Self-Diffusion Measurements. All the measurements were performed at 20 ± 0.1 °C. To obtain a series of diffusion coefficients during the coagulation process, the self-diffusion of the molecule studied was first measured in the casein suspension. After the addition of chymosin, the sample was rapidly prepared and placed in the spectrometer, and the diffusion experiment was performed again without any changes in the sequence parameters and allowed to repeat over the course of time.

Water self-diffusion was measured on a 20 MHz Bruker spectrometer equipped with a field gradient probe with a spin echo sequence (PFG-SE). The NMR tubes had an internal diameter of 8 mm, and calibration of the strength of gradients was performed with a sample of pure water of a known self-diffusion coefficient at 20 °C ($D_{H_2O} = 1.98 \times 10^{-9}$ m^2·s^{-1}). Ten values of the gradient strength (g) ranging between 0.6 and 3.2 T/m were used during each measurement. Four scans were carried out and the recycle delay was set at five T_1. The gradient length (δ) and the diffusion interval (Δ) were 0.5 and 5.0 ms, respectively.

PEG self-diffusion measurements were performed on a 500 MHz Bruker spectrometer equipped with a field gradient probe with 5 mm NMR tubes. Diffusion spectra were acquired with a stimulated echo sequence using bipolar gradients (STE-BP) and a 3−9−19 WATERGATE pulse scheme to suppress the water signal. Experiments were carried out with 16 different values of g, ranging from ∼0.25 to 5.00 T/m, and with a gradient length (δ) of 1.0 ms. Sixteen scans were carried out and the recycle delay was set at three T_1. Depending on the molecular weight of the PEG studied, Δ was adjusted to obtain a diffusion distance $z \sim 1.5$ μm in the casein suspension, in accordance with the Einstein equation $z = (2 D_{PEG}\Delta)^{1/2}$. This procedure enabled molecular probes to cover a much greater distance than the casein micelle diameter (diameter around 150 nm[32]).

NMR Processing Methods. All the data processing was performed with Matlab software. Monte Carlo simulations were used for error calculations with 200 iterations, in agreement with the procedures described by Alper and Gelb (1990).[33] In a PFG−NMR sequence, the echo intensity of a single molecule (I) is described by

$$I/I_0 = \exp(-kD) \tag{1}$$

where I_0 is the signal intensity in the absence of gradients and D the self-diffusion coefficient of the molecule studied. The values taken by k in a classic spin echo sequence (as for water self-diffusion measurements) are given by the following equation:

$$k = \gamma^2 g^2 \delta^2 \Delta \tag{2}$$

However, in a STE-BP NMR sequence (as for PEG self-diffusion measurements) the equation is transformed into:

$$k = \gamma^2 g^2 \delta^2 (\Delta - \delta/3 - \tau/2) \tag{3}$$

Here, γ is the gyromagnetic ratio (for protons $\gamma = 26.7520 \times 10^7$ rad·T^{-1}·s^{-1}), g the amplitude of the gradient pulse, δ the gradient pulse duration, Δ the time between the leading edges of gradient pulses, and τ the time between the end of each gradient and the next radiofrequency pulse.

In an ordinary high-field NMR proton spectrum, the PEG peak overlaps with casein signals at a shift of ∼3.6 ppm. However, due

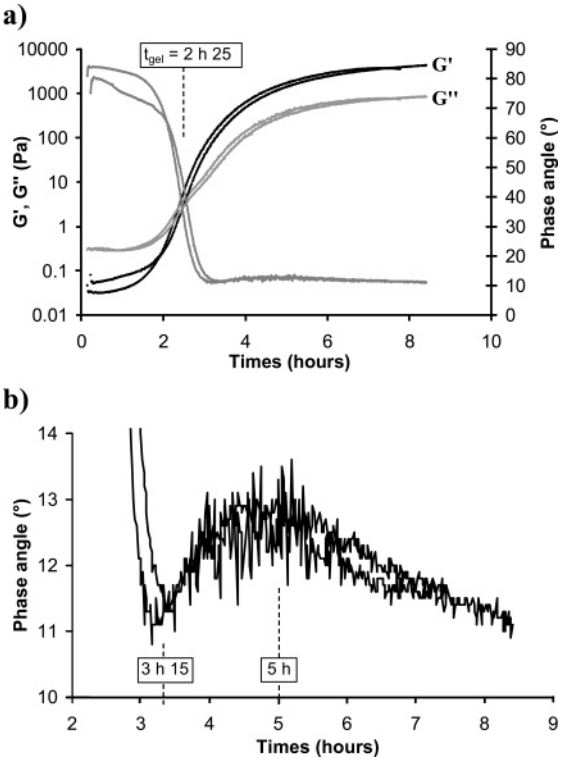

Figure 1. Rheological data according to time after addition of chymosin (two repetitions): (a) Evolution of storage modulus (G'), loss modulus (G'') and phase angle (δ); (b) Enlargement of phase angle evolution.

Table 2. Textural Properties of the Enzymatic Gel at Different Times after Addition of Chymosin at 20 °C

time after the chymosin addition	stiffness (N/mm)	hardness (N)	strength at fracture (N)
3h47	0.023	0.27	
4h34	0.081	0.9	
5h19	0.151		0.85 at 4.7 mm
5h58	0.214		1.15 at 4.7 mm
6h42	0.256		1.39 at 4.8 mm
7h08	0.321		1.65 at 4.8 mm

to the very short relaxation times (T_1, T_2) of casein protons, their signals were severely attenuated in the diffusion spectra and did not contribute to the PEG echo intensity. Casein signals were therefore always ignored and all self-diffusion coefficients were obtained by fitting eq 1 to the raw NMR data using nonlinear least-square methods.

Results

Rheological Parameters. The storage modulus (G'), the loss modulus (G'') and the phase angle (δ) recorded during the coagulation process are given in Figure 1a for two repetitions. The transition from solution to gel occurred between approximately $t = 2$ and 3 h. The time at which G' and G'' were equal is often used to define the "gel time" parameter. In this study, it was found to be $t_{gel} = 2$ h 25 ± 3 min. Although the phase angle was relatively stable after the sol−gel transition (from $t \sim 3$ h 15), which is characteristic of a type of structural organization, G' and G'' continued to increase (see Figure 1a). This indicated an increase in the gel stiffness consistent with the increasing values measured with the penetration tests shown in Table 2. As expected, the hardness, or the strength at fracture when it occurred, also increased during this interval. It can be concluded from all these rheological findings that the junctions in the network became progressively stronger after gel formation. Besides these general trends, as illustrated in Figure 1b, the curve representing the phase angle over time was not totally flat after the sol−gel transition. Just after aggregation (at $t \sim 3$ h 15) a local minimum in the phase angle occurred, indicating that the viscoelastic properties of the fresh gel were not totally stable. Such a phenomenon is therefore generally attributed to a transient gel structure. After this small reduction in gel elasticity (beyond $t \sim 5$ h) the phase angle gently decreased again to more elastic values.

SEM Images. SEM images of the gel are shown at different times after enzyme addition in Figure 2. As can be seen from Figure 2, parts a, c, and e, the gel microstructure appeared homogeneous at a length scale of a few micrometers. Parts a and b of Figure 2 show that the network soon after gel formation was constituted of casein aggregates composed of small spherical particles with a mean diameter around 100−150 nm. At this point the gel was coarse, with small pores. At $t = 8$ h 45, the network organization was very similar, but larger empty spaces were observed at the same time, indicating that the gel structure had evolved (Figure 2, parts c and d). Finally, 24 h after the addition of chymosin, the microstructure appeared clearly more branched (Figure 2, parts e and f). The casein particles had partially fused together, thin strands were formed and pore sizes were increased. A clear evolution of the network toward a more "open" microstructure was thus observed during the hours following gel formation.

Self-Diffusion in Water and Casein Suspensions. The diffusion coefficients of water and the two PEGs were carefully measured in a H_2O/NaCl solution (0.1 M) and in the casein suspension before the dynamic studies. The results obtained are presented in Table 3 with the polydispersity index of each polymer. The diffusion coefficients obtained in water were in good agreement with previous studies[11,30,31,34] and, as both PEGs were fairly monodisperse, all the echo attenuations were linear, indicating that there was no need to account for polydispersity effects. Such linear behavior was always observed in this study. Reduced self-diffusion coefficients (D_R) in the casein suspension were calculated to highlight the casein obstruction effect. They were obtained by dividing the self-diffusion coefficient in the casein suspension (D) by that in water (D_0). As can be seen from Table 3, the hindrance of diffusion by casein micelles was greater when molecules were larger. These findings are consistent with previous studies in which the casein powder was rehydrated in D_2O.[30,31]

Stability of the Repeated Self-Diffusion Experiments. To follow the evolution of a diffusion coefficient during the coagulation process, NMR self-diffusion experiments were repeated over a long period of time. The time-stability of this procedure was therefore beforehand verified. Normalized self-diffusion coefficients obtained for H_2O at 20 MHz and the 620 g/mol PEG at 500 MHz in a 0.1 M NaCl/H_2O solution are presented in Figure 3 in relation to time. At both 20 and 500 MHz, the mean values remained stable for all experiments, thus demonstrating that no drift occurred with time. In addition, good repeatability was found for both types of diffusion experiment as the standard deviations were 0.5% and 1.04% at 20 and 500 MHz, respectively. All these findings indicate that, in contrast to small variations between two nearby points, durable changes in the mean value of diffusion coefficients cannot be attributed to the measurement process itself.

Molecular Self-Diffusion During Casein Coagulation. The self-diffusion coefficient of each PEG and H_2O in the casein suspension (D_{sol}) was used to normalize all self-diffusion coefficients obtained during the coagulation process. The dilution induced by the inoculation of chymosin was ignored

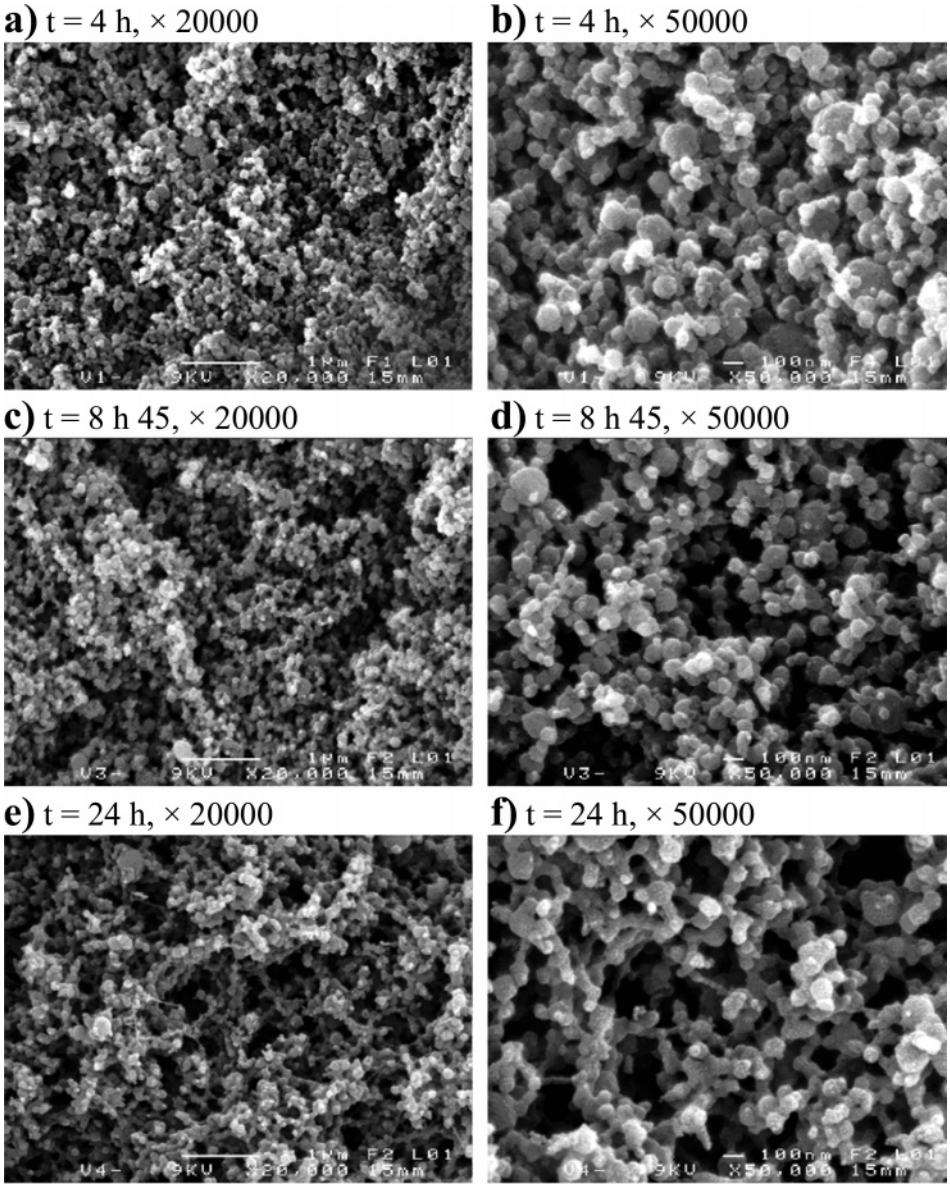

Figure 2. SEM images of enzymatic gels at two magnifications (× 20 000 and × 50 000) and at different times after addition of chymosin: (a and b) $t = 4$ h; (c and d) $t = 8$ h 45; (e and f) $t = 24$ h.

Table 3. Self-Diffusion Coefficients (D_0) and Reduced Self-diffusion Coefficients (D_R) of the Molecules Studied at 20 °C in a H_2O/NaCl Solution (0.1 M) and in a Casein Suspension of 15 g of Casein per 100 g of Water, Respectively

diffusing molecule	M_w/M_n	D_0 ($m^2 \cdot s^{-1}$)	$D_R = D/D_0$
H_2O		1.98×10^{-9}	0.71
PEG 620 g/mol	1.06	2.67×10^{-10}	0.63
PEG 96750 g/mol	1.06	1.61×10^{-11}	0.34

as the amount added was only about 0.7% of the total sample mass.

The results obtained for the diffusion of water are illustrated in Figure 4. As previously reported,[31,35] our findings suggest that the diffusion rate of H_2O was unaffected by the coagulation process. The variations in the diffusion coefficient observed with time were most probably caused by evaporation-condensation phenomena as tiny water drops were found on the tube wall at the end of the experiment.

The results obtained during the coagulation process for the 96750 g/mol PEG are presented in Figure 5 in relation to time after the addition of enzyme. Two different phases clearly appeared. During the first period (from $t = 0$ to about 5 h) the diffusion coefficient of the polymer remained stable. During the second period it then regularly increased with time. After 24 h, the diffusion coefficient was enhanced by approximately 20%, which is consistent with results previously reported in casein gels made with heavy water.[30,31]

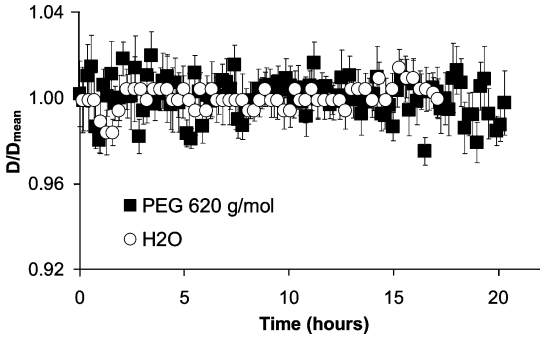

Figure 3. Repeated self-diffusion measurements in a 0.1 M NaCl/H_2O solution at 20 °C. The diffusion coefficients of H_2O and the 620 g/mol PEG were obtained at 20 and 500 MHz, respectively. Error bars represent the uncertainties given by the Monte Carlo simulations.

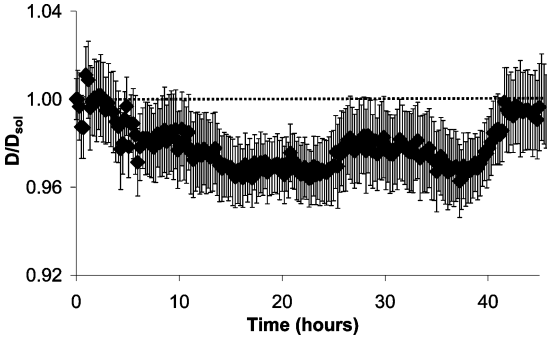

Figure 4. Evolution of self-diffusion coefficient of H_2O over time after addition of chymosin. Measurements were performed at 20 °C and 20 MHz. Error bars represent the uncertainties given by the Monte Carlo simulations.

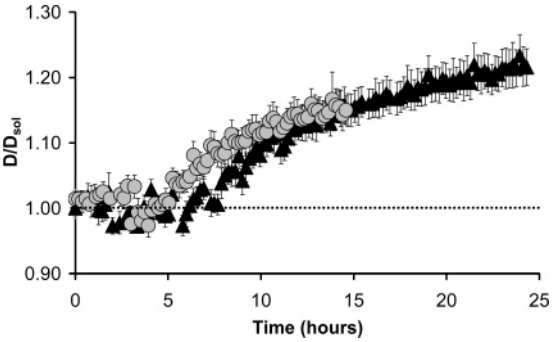

Figure 5. Evolution of 96750 g/mol PEG self-diffusion coefficient over time after addition of chymosin. Measurements were performed at 20 °C and 500 MHz. Circles and triangles are repetitions and error bars represent the uncertainties given by the Monte Carlo simulations.

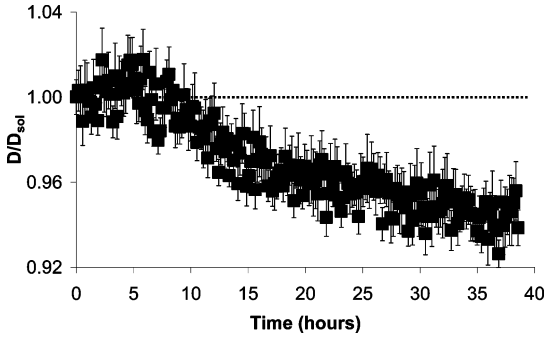

Figure 6. Evolution of 620 g/mol PEG self-diffusion coefficient over time after addition of chymosin. Measurements were performed at 20 °C and 500 MHz. Error bars represent the uncertainties given by the Monte Carlo simulations.

In fact, despite the smaller extent of variations, the opposite trend was found for the 620 g/mol PEG (Figure 6). Between $t = 0$ and about 5 h, the diffusion coefficient of the polymer was unchanged, but beyond this period a small and regular decrease in the diffusion rate was observed. Note that evaporation phenomena cannot explain this latter result because this phenomenon was never observed in samples analyzed at 500 MHz. This is understandable because the surface area in the NMR tube used (5 mm instead of 10 mm at 20 MHz) was very small compared to the total sample volume. Moreover, such an interpretation would hardly explain the shape of the curve.

Discussion

Characterization of the Coagulation Process. The coagulation induced by chymosin action is generally broken down into three phases: enzyme action, aggregation and gel aging.[36,37] First, the enzyme specifically splits off the κ-casein which is at the surface of the supramolecular edifice. This reduces the steric and electrostatic repulsions between the casein particles and the suspension becomes unstable. In the second phase, the resulting para-casein micelles spontaneously aggregate and form a macroscopic network. In this study, this phenomenon was characterized by the rapid increase in G' and G'' and the sudden decrease in δ between $t \sim 2$ h and $t \sim 3$ h 15 (Figure 1). Finally, the third phase corresponds to the aging of the gel and is characterized by the occurrence of structural changes in the casein network. This latter phase is of primary importance because it is common to all casein gels, and also because the gel microstructure is directly related to the physical characteristics of the product. Although the nature of the stages is different, they are not clearly separated in time. The aggregation phase always starts before the end of the enzymatic reaction[38,39] and occurs at an even lower degree of κ-casein hydrolysis when the casein concentration is increased.[37,40]

According to our findings, the gel aging phase was characterized by an increase in gel stiffness (Table 2) consistent with the evolutions of G' and G'' (Figure 1a). In addition, the gel microstructure became progressively more "open" as shown by the SEM images (Figure 2), indicating that the casein particles had fused together and progressively became more compact. All these findings are in agreement with the literature.[1,6,41] To describe this particular phase, Mellema et al.[1] proposed a general model based on several types of rearrangement occurring at different length scales. According to them, particle fusion and inter-particle rearrangements result in the formation of straight and progressively thinner strands, with more bonds per casein aggregate, and hence stronger junctions. This consequently leads to stretching of strands and stiffening of the gel.[1] Although the mechanisms involved are not fully understood, all authors agree that rearrangements give rise to local matrix fusion and compaction, resulting in a gel with larger pores and a higher permeability.[1,2,4,6,37,41−43] After network establishment, the progressive reorganization of the gel microstructure is thus accompanied by a reduction in the amount of water contained in casein particles; the aggregates become denser.

Background on Self-Diffusion in Casein Samples. Previous studies have shown that probe diffusion in casein suspensions and gels is greatly dependent on both the volume fraction occupied by casein particles and the probe size.[30,31] The reduction in diffusion coefficient for a given volume fraction of casein particles is smaller for smaller probes (e.g., Table 3). This phenomenon was previously explained by assuming a model with two diffusion pathways, one around and one through the casein micelles.[30] According to the "two site" model, variations in the diffusion rate of a molecule only depend on its ability to diffuse through the casein particles and the volume fraction occupied by them (see refs 30 and 44 for more details). This model therefore implies that the diffusion of larger molecules is more affected by the presence of casein particles because they can less easily diffuse through them (Table 3). This means that the "through the casein particles" diffusion component for the 96750 g/mol PEG is much smaller than those for water and the small PEG. Such an explanation was proposed because casein particles cannot be considered as impenetrable particles since they are known to be very porous and highly hydrated. Indeed, casein micelles are generally reported to be constituted of approximately 3 or 4 g of water per 1 g casein,[45−49] and several studies have shown that large molecules such as β-casein (24000 g/mol)[50,51] and transglutaminase (45000 g/mol)[52−55] can enter a casein micelle.

To explain the probe size dependence, another approach consistent with the one given above can be proposed on the basis of the recent results obtained by Babu et al.[56] They showed by computer simulations that the diffusion of a spherical probe in hard sphere suspensions and gels is mainly dependent on the volume fraction that is accessible to the diffusing particle. According to this interpretation, the diffusion of larger probes would thus be more affected in the presence of casein particles because they have a smaller accessible volume fraction. It should be noted that the situation was slightly different in this study as PEGs are easily deformable and can change their shape according to their environment.[57,58] They can therefore diffuse through small spaces compared to their hydrodynamic diameter by adopting a more elongated conformation. Although this phenomenon complicates the modeling of diffusion data, we may suppose that the following two assumptions are still tenable:

- The accessible volume fraction is a key parameter to explain our diffusion results.
- The volume fractions that are accessible to the molecules studied are different.

In addition to PEG flexibility, the three molecules used in this study are much smaller than casein particles, which have a mean diameter around 150 nm.[32] The accessible volume surrounding the casein particles should therefore be of the same order of magnitude for water and both PEGs. The differences between the volume fractions which are accessible to the molecules investigated would thus be mainly explained by different amounts of accessible space inside the casein particles. As previously stated, this latter interpretation is thus very consistent with the previous interpretation.

Self-Diffusion During the Coagulation Process. As shown in Figures 4−6, different evolutions in the diffusion rate of the molecules studied occurred during the coagulation process. The diffusion of water remained stable throughout the experiment while those of both PEGs started to change after approximately 5 h of coagulation. Moreover, the diffusion coefficient of the small PEG progressively decreased whereas the opposite occurred for the large PEG. These results were unexpected because we have to consider that the same causes can lead to different evolutions of diffusion rates depending on the molecular weight of the probe. In other words, the diffusing molecules did not experience the same phenomena because of their different sizes. Scaling effects must therefore be considered.

At $t \sim 5$ h, the formation of the macroscopic network was complete (Figure 1). The changes in both PEG diffusion rates observed should therefore be a consequence of the rearrangement processes that occur during gel aging (Figures 5 and 6). As previously described, this phase was characterized by a compaction of the obstructing elements and hence a reduction in the amount of water contained by the casein particles (Figure 2). According to the "two site" model, this phenomenon should have two opposite effects on the diffusion of probes. On the one hand, more molecules should freely diffuse because more empty spaces are created inside the gel microstructure. This should result in an enhanced diffusion coefficient. On the other hand, the "through the casein aggregates" diffusion component would be expected to decrease as they become denser, and this should lead to a reduction in the diffusion rate. Note that exactly the same conclusions can be reached in terms of accessible volume fraction by distinguishing the accessible volumes which are outside the casein particles from those which are inside. By following this interpretation, it becomes possible to explain how probe diffusion coefficients can vary differently depending on the size of the diffusing molecule and hence on the length scale probed.

First of all, the diffusion rate of water molecules remained stable throughout the coagulation process as evaporation-condensation phenomena explain the instability observed (Figure 4). Water diffusion was thus not affected by the changes in the casein particle structure nor by the reduction in casein network volume. The obstruction effect seemed therefore to be explained by the proteins themselves and water molecules should be considered as "point particles", i.e. the volume fraction that is accessible to water does not depend on the matrix structure. These findings confirm previously reported results obtained in casein[35] and in whey protein[59] matrices since they were fully explained by the protein content and their local interactions with water.

The diffusion coefficient of the 96750 g/mol PEG progressively increased with time after $t \sim 5$ h (Figure 5). Its diffusion rate was thus mainly affected by the progressive increase in the casein-free volume. This is understandable because in the suspension its diffusion coefficient was severely reduced compared to those of water and the small polymer (Table 3). It would therefore be dangerous to make assumptions regarding the ability of this large PEG to diffuse through casein particles. If it cannot, the interpretation is straightforward. The self-diffusion coefficient of this polymer can only increase because the volume fraction that is accessible to this probe increases when the volume occupied by the obstructing elements decreases. If this polymer can in fact diffuse through casein particles, this diffusion component must be small and may therefore not be significantly further reduced when the casein aggregates become denser. The effect produced by the progressive increase in the casein-free volume fraction may thus still prevail. Whatever the case, the results presented in Figure 5 clearly demonstrate that the diffusion rate of the 96750 g/mol PEG was very sensitive to the reduction in the casein particle water content, and hence to the progressive increase in gel porosity.

Turning to the small probe results, the reduced diffusion coefficient of the 620 g/mol PEG in casein suspension was slightly smaller than that of water (Table 3). We can therefore also assume a diffusion behavior with two diffusion pathways. However, in contrast to what was observed for water and the large PEG, a small decrease in the diffusion rate of the 620 g/mol PEG progressively occurred after $t \sim 5$ h (Figure 6). According to the two site model, despite the increase in the casein-free volume, the "through the casein aggregates" diffusion component was sufficiently reduced to induce a decrease in the overall diffusion coefficient. This leads to the interesting conclusion that when casein aggregates become denser, the consequent reduction in the "through the casein aggregates" diffusion component is greater for the polymer than for water. This appears to be logical because the diffusion of this PEG was already more hindered than that of water in the casein suspension (Table 3). The evolution of the 620 g/mol PEG self-diffusion coefficient seems therefore to be sensitive to phenomena occurring inside the casein aggregates and thus to their structure.

It is noteworthy that, in general, the casein aggregate compaction might not be the only factor influencing probe diffusion. Indeed, network densification is a consequence of structural rearrangements on a micrometric scale, but other effects necessarily occur at smaller levels including the molecular scale.[60,61] At such length scales (i.e., inside particles), and without considering protein crowding, it is not possible to

determine what the impact of the structural rearrangement processes on molecular diffusion might be. The 620 g/mol PEG diffusion could therefore also be sensitive to other phenomena. Similarly, and particularly for molecules which cannot enter casein particles, in addition to casein-free volume variations (i.e., porosity effects), changes in the pore connectivity (i.e., tortuosity effects) should also rigorously be considered. Nevertheless, we can be confident that the main phenomenon explaining our diffusion results was the progressive network compaction, both because of its extent (Figure 2) and because the curves obtained for the small and the large PEG were remarkably symmetric.

However, the diffusion of the three molecules studied was unaffected by the first two stages of coagulation, i.e., the enzymatic and the aggregation phases (Figure 4−6). During the first stage, chymosin cleaves out one part of each κ-casein from the surface of the casein micelles. This results in a small reduction in their mean diameter (around 15 nm[38,62,63]) but, according to Sandra et al.,[38] no significant changes occur in the internal structure of casein particles. This is consistent with our findings, since the structure of the colloidal particles did not seem to be affected at the scale probed by the 620 g/mol PEG during the enzymatic reaction. Such a decrease in particle size could also be thought to result in an increase in the 96750 g/mol PEG diffusion rate, but this reasoning would overlook the fact that the obstacles removed are released in the serum phase. The noninfluence of the aggregation step can also be easily explained. Indeed, according to the concentration used and the micelle size, when compared to the PEG diffusion coefficients, casein micelles can already be considered as static in the suspension.

After aggregation (from $t \sim 3$ h 15 to $t \sim 4$ h) the continuous increase in G' and G'' (Figure 1a) and the evolution of δ (Figure 1b) indicate that structural changes occurred as soon as a gel was formed. These findings are consistent with the fact that the different phases of the coagulation are not clearly separate in time, but they also imply that the reduction in casein water content did not start simultaneously with the structural rearrangement processes. However, at $t \sim 5$ h, when both PEG diffusion rates started to vary, the evolution in the phase angle changed again (Figure 1b). Such a small and progressive decrease in the phase angle is usually difficult to analyze but, according to our findings, although this phenomenon is necessarily caused by a structural reorganization inside the particles, it seems to be linked to a gradual reduction in the casein volume fraction.

Conclusions

We revealed by an original designed experiment that probe diffusion measurements can give dynamic information regarding the structural modifications that take place during the gel aging phase of a casein coagulation process. Moreover, depending on the size of the diffusing molecule, information could be obtained at different length scales. Water diffusion was only affected by protein content and not by changes in the structure of the casein aggregates, in contrast to the diffusion of a 620 g/mol PEG. The diffusion of a 96750 g/mol PEG was not affected by the sol−gel transition but was closely related to the progressive rise in gel porosity. These findings show the importance of the rearrangement processes to explain milk gel properties.

PFG−NMR and viscoelastic investigations were found to be highly complementary. For example, we showed that the progressive compaction of casein aggregates did not directly start after gel formation and was probably related to a small and gradual decrease in the phase angle. Moreover, few techniques exist to study the evolution of fresh gel properties and most of them are invasive and non-continuous, as for instance permeametry experiments which provide information regarding gel permeability. In contrast, repeated probe diffusion measurements are easy to set up, and both the extent and the rate at which the network compaction increase can be estimated in only one run. It may therefore become a valuable tool to study the impact of various parameters on rearrangement processes.

Probe diffusion measurements during the coagulation processes induced by acidification alone and with the concomitant action of chymosin are in progress to obtain further insight regarding these phenomena.

Acknowledgment. The authors thank the Regional Council of Brittany and SOREDAB for financial support. We are grateful to Armel Guillermo and Arnaud Bondon for their help with NMR experiments and Joseph Le Lannic for assistance with the SEM experiments. We thank Jean-Michel Soulié; Sandrine Eliot-Godéreaux; Pascale Persenot and Fabien Guitter from SOREDAB for helpful discussions and assistance with the rheological and mechanical experiments, and Minale Ouethrani for participating in the rheological and SEM experiments.

References and Notes

(1) Mellema, M.; Walstra, P.; Van Opheusden, J. H. J.; Van Vliet, T. *Adv. Colloid Interface Sci.* **2002**, *98*, 25−50.
(2) Lagoueyte, N.; Lablee, J.; Lagaude, A.; Delafuente, B. T. *J. Food Sci.* **1994**, *59*, 956−959.
(3) Lucey, J. A.; van Vliet, T.; Grolle, K.; Geurts, T.; Walstra, P. *Int. Dairy J.* **1997**, *7*, 381−388.
(4) Lucey, J. A.; Tamehana, M.; Singh, H.; Munro, P. A. *Int. Dairy J.* **2001**, *11*, 559−565.
(5) Aichinger, P. A.; Michel, M.; Servais, C.; Dillmann, M. L.; Rouvet, M.; D'Amico, N.; Zink, R.; Klostermeyer, H.; Horne, D. S. *Colloids Surf. B: Biointerfaces* **2003**, *31*, 243−255.
(6) Mellema, M.; Heesakkers, J. W. M.; van Opheusden, J. H. J.; van Vliet, T. *Langmuir* **2000**, *16*, 6847−6854.
(7) Lucey, J. A.; Tamehana, M.; Singh, H.; Munro, P. A. *Food Res. Int.* **1998**, *31*, 147−155.
(8) Van, Vliet, T.; Lakemond, C. M. M.; Visschers, R. W. *Curr. Opin. Colloid Interface Sci.* **2004**, *9*, 298−304.
(9) Mishra, R.; Govindasamy-Lucey, S.; Lucey, J. A. *J. Texture Studies* **2005**, *36*, 190−212.
(10) Lopez, M. B.; Lomholt, S. B.; Qvist, K. B. *Int. Dairy J.* **1998**, *8*, 289−293.
(11) Johansson, L.; Shantze, U.; Lofroth, J. E. *Macromolecules* **1991**, *24*, 6019−6023.
(12) Johansson, L.; Elvingson, C.; Lofroth, J. E. *Macromolecules* **1991**, *24*, 6024−6029.
(13) Masaro, L.; Ousalem, M.; Baille, W. E.; Lessard, D.; Zhu, X. X. *Macromolecules* **1999**, *32*, 4375−4382.
(14) Brown, W.; Stilbs, P. *Polymer* **1982**, *24*, 188−192.
(15) Walderhaug, H.; Nystrom, B. *Colloids Surf. A: Physicochem. Eng. Asp.* **1999**, *149*, 379−387.
(16) Petit, J. M.; Zhu, X. X.; Macdonald, P. M. *Macromolecules* **1996**, *29*, 70−76.
(17) Jo, B. W.; Hess, M.; Zahres, M. *Mater. Res. Innovations* **2003**, *7* (3), 178−182.
(18) Matsukawa, S.; Ando, I. *Macromolecules* **1996**, *29*, 7136−7140.
(19) Matsukawa, S.; Ando, I. *Macromolecules* **1997**, *30*, 8310−8313.
(20) Fleischer, G.; Karger, J.; Rittig, F.; Hoerner, P.; Riess, G.; Schmutzler, K.; Appel, M. *Polym. Adv. Technol.* **1998**, *9*, 700−708.
(21) Yamane, Y.; Ando, I.; Buchholz, F. L.; Reinhardt, A. R.; Schlick, S. *Macromolecules* **2004**, *37*, 9841−9849.
(22) Amsden, B. *Macromolecules* **1998**, *31*, 8382−8395.
(23) Baldursdottir, S. G.; Kjoniksen, A.-L.; Nystrom, B. *Eur. Polym. J.* **2006**, *42*, 3050−3058.
(24) Amsden, B. *Macromolecules* **2001**, *34*, 1430−1435.
(25) Kwak, S.; Lafleur, M. *Colloids Surf. A: Physicochem. Eng. Asp.* **2003**, *221*, 231−242.
(26) Nyden, M.; Soderman, O.; Karlstrom, G. *Macromolecules* **1999**, *32*, 127−135.
(27) Croguennoc, P.; Nicolai, T.; Kuil, M. E.; Hollander, J. G. *J. Phys. Chem. B* **2001**, *105*, 5782−5788.

(28) Colsenet, R.; Soderman, O.; Mariette, F. *J. Agric. Food Chem.* **2006**, *54*, 5105−5112.
(29) Colsenet, R.; Soderman, O.; Mariette, F. O. *Macromolecules* **2006**, *39*, 1053−1059.
(30) Colsenet, R.; Soderman, O.; Mariette, F. *Macromolecules* **2005**, *38*, 9171−9179.
(31) Le Feunteun, S.; Mariette, F. *J. Agric. Food Chem.* **2007**, *55*, 10764−10772.
(32) McMahon, D. J.; Brown, R. J. *J. Dairy Sci.* **1984**, *67*, 499−512.
(33) Alper, J. S.; Gelb, R. I. *J. Phys. Chem.* **1990**, *94*, 4747−4751.
(34) Masaro, L.; Zhu, X. X.; MacDonald, P. M. *J. Polym. Sci., Part B: Polym. Phys.* **1999**, *37*, 2396−2403.
(35) Mariette, F.; Topgaard, D.; Jönsson, B.; Söderman, O. *J. Agric. Food Chem.* **2002**, *50*, 4295−4302.
(36) Zoon, P.; Van Vliet, T.; Walstra, P. *Neth. Milk Dairy J.* **1988**, *42*, 249−269.
(37) Karlsson, A. O.; Ipsen, R.; Ardo, Y. *Int. Dairy J.* **2007**, *17*, 674−682.
(38) Sandra, S.; Alexander, M.; Dalgleish, D. G. *J. Colloid Interface Sci.* **2007**, *308*, 364−373.
(39) Walstra, P.; Van Vliet, T. *Neth. Milk Dairy J.* **1986**, *40*, 241−259.
(40) Sharma, S. K.; Mittal, G. S.; Hill, A. R. *Milchwissensch. Milk Sci. Int.* **1994**, *49*, 450−453.
(41) Bauer, R.; Hansen, M.; Hansen, S.; Ogendal, L.; Lomholt, S.; Qvist, K.; Harne, D. *J. Chem. Phys.* **1995**, *103*, 2725−2737.
(42) Lucey, J. A.; van Vliet, T.; Grolle, K.; Geurts, T.; Walstra, P. *Int. Dairy J.* **1997**, *7*, 389−397.
(43) Lucey, J. A.; Tamehana, M.; Singh, H.; Munro, P. A. *J. Dairy Res.* **2000**, *67*, 415−427.
(44) Jönsson, B.; Wennerstrom, H.; Nilsson, P. G.; Linse, P. *Colloid Polym. Sci.* **1986**, *264*, 77−88.
(45) Kumosinski, T. F.; Pessen, H.; Farrell, H. M., Jr.; Brumberger, H. *Arch. Biochem. Biophys.* **1988**, *266*, 548−561.
(46) Guillaume, C.; Jimenez, L.; Cuq, J. L.; Marchesseau, S. *Int. Dairy J.* **2004**, *14*, 305−311.
(47) Gastaldi, E.; Lagaude, A.; Marchesseau, S.; DelaFuente, B. T. *J. Food Sci.* **1997**, *62*, 671.
(48) Vetier, N.; Banon, S.; Ramet, J. P.; Hardy, J. *Lait* **2000**, *80*, 237−246.
(49) Karlsson, A. O.; Ipsen, R.; Schrader, K.; Ardo, Y. *J. Dairy Sci.* **2005**, *88*, 3784−3797.
(50) Dalgleish, D. G.; Law, J. R. *J. Dairy Res.* **1989**, *56*, 727−735.
(51) Creamer, K.; Berry, G. P.; Mills, O. E. *New Zeeland J. Dairy Sci. Technol.* **1997**, *12*, 58.
(52) De Kruif, C. G.; Tuinier, R.; Holt, C.; Timmins, P. A.; Rollema, H. S. *Langmuir* **2002**, *18*, 4885−4891.
(53) O'Connell, J. E.; De Kruif, C. G. *Colloids Surf. A: Physicochem. Eng. Aspects* **2003**, *216*, 75−81.
(54) Schorsch, C.; Carrie, H.; Clark, A. H.; Norton, I. T. *Int. Dairy J.* **2000**, *10*, 519−528.
(55) Schorsch, C.; Carrie, H.; Norton, I. T. *Int. Dairy J.* **2000**, *10*, 529−539.
(56) Babu, S.; Gimel, J.-C.; Nicolai, T. *J. Phys. Chem. B* **2008**, *112*, 743−748.
(57) De Gennes, P. G. *J. Chem. Phys.* **1971**, *55*, 572−579.
(58) De Gennes, P. G. *Nature (London)* **1979**, *282*, 367−370.
(59) Colsenet, R.; Cambert, M.; Mariette, F. *J. Agric. Food Chem.* **2005**, *53*, 6784−6790.
(60) Horne, D. S. *Int. Dairy J.* **1998**, *8*, 171−177.
(61) Horne, D. S. *Colloids Surf. A: Physicochem. Eng. Asp.* **2003**, *213*, 255−263.
(62) Alexander, M.; Dalgleish, D. G. *Colloids Surf. B: Biointerfaces* **2004**, *38*, 83−90.
(63) Dwyer, C.; Donnelly, L.; Buckin, V. *J. Dairy Res.* **2005**, *72*, 303−310.

MA702246M